Smart Structures and Systems, *Vol. 18, No. 1 (2016) 1-16*
DOI: http://dx.doi.org/10.12989/sss.2016.18.1.001

Dynamic transient analysis of systems with material nonlinearity: a model order reduction approach

F. Casciati* and L. Faravelli

Department of Civil Engineering and Architecture, University of Pavia, Via Ferrata 3, 27100 Pavia (PV), Italy

(Received September 26, 2015, Revised April 21, 2016, Accepted May 6, 2016)

Abstract. Model Order Reduction (MOR) denotes the theory by which one tries to catch a model of order lower than that of the real model. This is conveniently pursued in view of the design of an efficient structural control scheme, just passive within this paper. When the nonlinear response of the reference structural system affects the nature of the reduced model, making it dependent on the visited subset of the input-output space, standard MOR techniques do not apply. The mathematical theory offers some specific alternatives, which however involve a degree of sophistication unjustified in the presence of a few localized nonlinearities. This paper suggests applying standard MOR to the linear parts of the structural system, the interface remaining the original unreduced nonlinear components. A case study focused on the effects of a helicopter land crash is used to exemplify the proposal.

Keywords: helicopter; model order reduction; nonlinearity; soil structure interaction;vibration mitigation

1. Introduction

This paper consists of two main contributions. The extension of a standard Model Order Reduction (MOR) scheme, which holds for linear systems, to incorporate minor nonlinear components and its application to the specific technical problem of the estimation of the effects of a helicopter land crashing.

Helicopters are allowed to land everywhere there is enough operational space, if there is an authorization to do it on behalf of the responsible local authority. Nevertheless, to promote a sort of traffic regulation, "heli-surfaces" are designed and built inside urban nuclei. Heli-surface is a term that applies to any area of suitable dimensions for the landing and taking-off of helicopters. The organized infrastructure is commonly referred to as "heliport" or "helipad".

The design and construction of a heliport is a matter of specialists. The references (www.faa.gov, 2004, www.wdbg.org, 2008) provide the main specification and the expected performance. However, the focus of this paper is not on the design of the landing plate, but on the risk analysis associated with the heliport localization. Indeed, the landing area becomes a clustering of helicopter trajectories, which implies a local increase of the probability of occurrence of the event "land-crash". Due to the large variety of helicopter features, such a risk problem cannot be approached by a global numerical model. It has to be managed by studying different

*Corresponding author, Professor, E-mail: fabio@dipmec.unipv.it

http://www.techno-press.org/?journal=sss&subpage=8 ISSN: 1738-1584 (Print), 1738-1991 (Online)

scenarios and by assigning to each studied event the corresponding probability of occurrence (fas.org, 1999, Casciati and Faravelli 1991).

In this framework, one introduces a source event (the impact of the helicopter on the land, Figure 1) and studies the likely consequent economical losses induced on third parties property. Since one is operating inside urban nuclei, the likely scenarios see the propagation of waves induced by the impact toward the surrounding buildings. Thus, the acceleration wave propagation, along the soil surface, has to be estimated by a numerical model of the whole system.

The structural system to be studied is made by the landing plate and the sub-standing soil. The latter one represents the vibration propagation medium as in a standard soil-structure interaction problem. The associated numerical model is built by a finite element discretization (Casciati and Borja 2004, Casciati and Osman 2005). Its dimension is usually significant, because several tens meters in depth and a few kilometres in the longitudinal and transversal horizontal directions have to be covered. This is mainly true if the actual nature of the material layers is considered. Two models reduction policies are therefore advocated when repeated analyses are required by the design of control strategies (Basu *et al*. 2014, Casciati *et al*. 2014) or by design optimization schemes (Casciati 2014):

1) Physical considerations allow one a first reduction by introducing equivalent material layers and by estimating the decay distance of the propagating wave.
2) A further, more significant, reduction is achieved by re-writing the governing equation in a balanced format where a truncation is easily introduced (Casciati and Faravelli 2014).

The second reduction is limited to problems with linear features. Much more complex schemes apply when nonlinear systems have to be studied (Casciati and Casciati 2006, Casciati and Faravelli 2012, Farhat *et al*. 2014, Farhat *et al*. 2015).

In the heliport analysis, however, the nonlinearity is just around the landing plate or at the interface between the landing plate and the soil. This suggested to investigate a procedure where model order reduction is strictly limited to subsets of linear equations preserving the whole nonlinear components.

Fig. 1 Helicopter impact on the land: the source event for the acceleration wave-propagation problem studied in the paper

2. Problem formulation

A general heli-surface is made by a plate of circular shape (marked by a capital H plus alphanumerical coded characters related to weight and rotor diameter limits). The plate is linked to the soil by some foundation elements. It is assumed here that the foundation is made by a given number of pillars, each of them ending in its own plinth.

Without any conceptual limitation, one studies the land-crash on the plate of a helicopter whose control is lost at a given height when the velocity components were known.

A finite element model using hexahedral elements for both soil and landing structure is built. Its physical reduction consists of two steps:

1) the extension of the soil surrounding the plate, originally up to the rock all around, is reduced and suitable fictitious boundary conditions are introduced. The driving criterion is that the wave caused by an impact dissipates inside the reduced soil and no reflection on the boundary occurs;
2) the material dis-homogeneity is considered by suitable local homogenization. In this case the driving criterion is that, within the top layers, the kinematic response to the impact be the same as the one estimated by the more detailed model.

At the end of the physical reduction, carried out within assumption of linear elastic constitutive laws, the static numerical models adopted in structural engineering consist of algebraic equations that account for the original partial differential equations of the continuum mechanics (FEA, i.e., finite element analysis). The dynamic system problem is then rearranged in terms of ordinary differential equations where the second derivative with respect to time appears. The number of equations represents the order of the model, say N.

2.1 Governing equations

Introducing the so-called state space representation, only linear derivatives of time are considered, with the number of equations being doubled. One writes

$$\dot{\boldsymbol{z}}(t) = \boldsymbol{A}\,\boldsymbol{z}(t) + \boldsymbol{B}\,\boldsymbol{u}(t) \tag{1}$$

where t denotes the time, $\boldsymbol{z}$ is the state variable vector of size $2N$, the superimposed dot denotes time derivative, $\boldsymbol{u}$ is the vector of the external excitations, of size p, and $\boldsymbol{A}$ and $\boldsymbol{B}$ are time invariant matrices of sizes $2N$ by $2N$ and $2N$ by p, respectively. The state variables are not supposed to have any physical meaning. But they are linked to any set of observables variables $\boldsymbol{y}(t)$ (denoted as "observed variables") by a second set of equations, this time of the algebraic type

$$\boldsymbol{y}(t) = \boldsymbol{C}\,\boldsymbol{z}(t) + \boldsymbol{D}\,\boldsymbol{u}(t) \tag{2}$$

An often-met situation sees the vector $\boldsymbol{y}$ ordered to give N (relative to the base) displacements followed by N (relative) velocities, so that, if $\boldsymbol{z}$ coincides with $\boldsymbol{y}$, $\boldsymbol{C}$ becomes an identity matrix of size $2N$ and $\boldsymbol{D}$ is assumed to be 0.

A further vector of length N can be computed as the vector of the (absolute) accelerations

$$\boldsymbol{y}_a(t) = -\left[(\boldsymbol{K}/\boldsymbol{M}) \quad (\boldsymbol{c}/\boldsymbol{M})\right]\boldsymbol{y}(t) \quad + (\boldsymbol{B}_{\text{bottom}} \quad /\boldsymbol{M})\boldsymbol{u}' \tag{3}$$

where $\boldsymbol{M}$, $\boldsymbol{c}$ and $\boldsymbol{K}$ are the matrices of mass, damping and stiffness, respectively. $\boldsymbol{B}_{\text{bottom}}$ denotes the last $2N$ row of matrix $\boldsymbol{B}$ in Eq. (1), while the first matrix in the equation makes explicit the nature of $\boldsymbol{A}$. $\boldsymbol{u}'$ denotes the actions not related to the base acceleration which is included in the l.h.s. of

Eq. (3).

Model reduction procedures are discrete versions of Ritz/Galerkin analyses: they seek solutions in the subspace generated by a transformation matrix $\boldsymbol{T}$ (Casciati and Faravelli 2014). Among different alternative schemes one adopts here the approach that re-writes Eq. (1) in a different basis system and applies to the obtained balanced system a truncation using Hankel singular values; the basis transformation also applies to Eq. (2) and after truncation just a bit of information is lost.

Equations from (1) to (3) can be re-written adding the suffix "*R*" (for reduced) to all the quantities, except the observed variables (Casciati and Faravelli 2014), when the reduced order model is pursued by balanced truncation

$$\dot{\boldsymbol{z}}_R(t) = \boldsymbol{A}_R\,\boldsymbol{z}_R(t) + \boldsymbol{B}_R\boldsymbol{u}(t) \tag{4}$$

$$\boldsymbol{y}(t) = \boldsymbol{C}_R\quad \boldsymbol{z}_R(t) \tag{5}$$

$$\boldsymbol{y}_a(t) = -[\boldsymbol{K}/\quad/\boldsymbol{M}]\,\boldsymbol{y}(t) + \boldsymbol{B}_{\text{bottom}}/\boldsymbol{M}\,\boldsymbol{u}' \tag{6}$$

The number of state variables is now *n*, with *n* significantly lower than 2*N*.

2.2 Proposed development

As discussed in (Casciati and Casciati 2016), the whole procedure and hence the suitable value of *n* is significantly affected by the size and nature of the matrix $\boldsymbol{C}$ as well as by the actual acceleration considered in the problem formulation.

Assume now that the structural problem contains localized material nonlinearities. Eq. (1) becomes

$$\dot{\boldsymbol{z}}(t) = \boldsymbol{A}\,\boldsymbol{z}(t) + \boldsymbol{B}(t)\quad + \boldsymbol{R}\,\boldsymbol{q}(t) \tag{7}$$

$$\boldsymbol{y}_{OB}(t) = \boldsymbol{C}_{OB}\,\boldsymbol{z}(t) \tag{8}$$

$$\boldsymbol{y}_{NL}(t) = \boldsymbol{C}_{NL}\,\boldsymbol{z}(t) \tag{9}$$

$$\boldsymbol{q}(t) = \boldsymbol{f}(\boldsymbol{u}(t), \boldsymbol{y}_{NL}(t)) \tag{10}$$

where the nonlinearities are accounted for the vector $\boldsymbol{q}$, related to the current state and the displacements $\boldsymbol{y}_{NL}$ in the nodes surrounding the nonlinearity domains. They are simply related to the state variables via the matrix $\boldsymbol{C}_{NL}$.

Eqs. (7)-(9) are linear and hence standard model order reduction applies

$$\dot{\boldsymbol{z}}_R(t) = \boldsymbol{A}_R\,\boldsymbol{z}_R(t) + \boldsymbol{B}_R(t) + \boldsymbol{R}_R\,\boldsymbol{q}(t) \tag{11}$$

$$\boldsymbol{y}_{OB}(t) = \boldsymbol{C}_{OB\,R}\,\boldsymbol{z}_R(t) \tag{12}$$

$$\boldsymbol{y}_{NL}(t) = \boldsymbol{C}_{NL\,R}\,\boldsymbol{z}_R(t) \tag{13}$$

$$\boldsymbol{q}(t) = \boldsymbol{f}(\boldsymbol{u}(t), \boldsymbol{y}_{NL}(t)) \tag{14}$$

The splitting of Eqs. (2) and (5) into the couples (8), (9) and (12), (13), respectively, requires an explanation. Eqs. (9) and its reduced version Eq. (13) outline the need of estimating those variables in view of their role in Eqs. (10) and (14), respectively. The index *OB* (i.e., observed) in Eqs. (8) and (12) emphasizes that a subset of all the nodes displacements and velocity is conveniently selected. Indeed, as it will be clarified within the following numerical example, the number of state variables in the reduced model is strongly influenced by the number of rows of

C_{OB}. In other words, an accurate catch of the response in many locations results in reduced order model with too many state variables, while an oculate selection of a few observed variables guarantee accuracy even with a very low number of reduced model state variables.

3. A case study exemplification

A real-case exemplification requires the availability of the structural design data as well as a deep knowledge of the soil below the heliport. The case study is located where the latter one is available. The source of information is often the webpage of the regional authority. Their format is not standardized and hence a site may show a better description than another.

3.1 Geometry and materials data: a first physical reduction

Fig. 2(a) shows a fine idealization of the soil along its depth. Alternate layers of clay, sand and silt are explicitly considered over a square of size 150 m, the deposit height being 100 m. Fig. 2(b) shows a less dense mesh where the layers come with "equivalent" material properties: here "equivalent" means that, under the gravity excitation and suitable horizontal actions, the top nodes show the same kinematic behaviour shown by the nodes in Fig. 2(a).

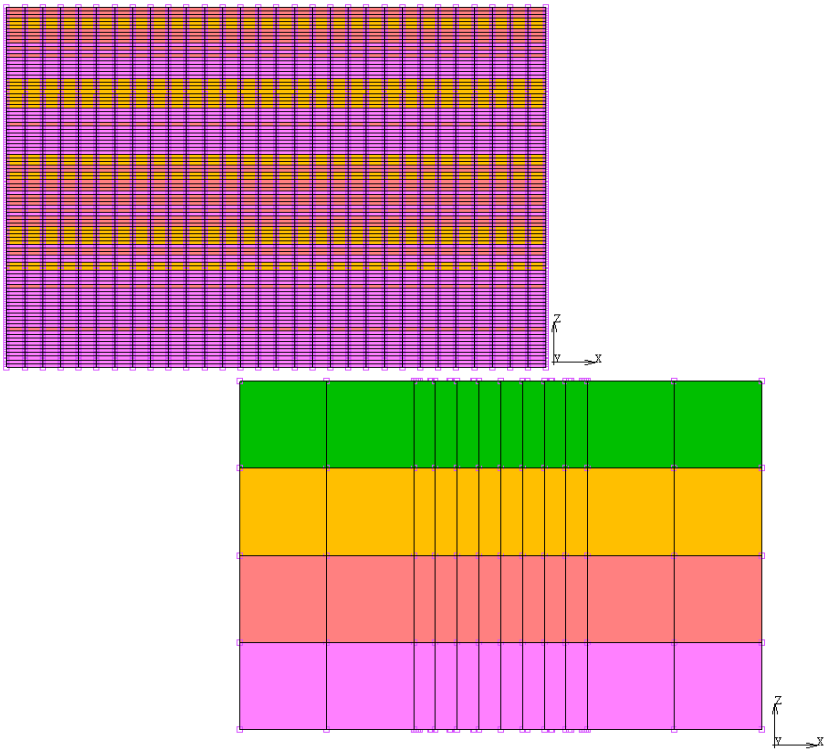

Fig. 2 Lateral view of a soil block of height 100 m; the base is a square 150 m by 150 m. (a) refined discretization accounting for the actual nature of the layers and (b) equivalent block description catching the same cinematic response with a lower number of degrees of freedom

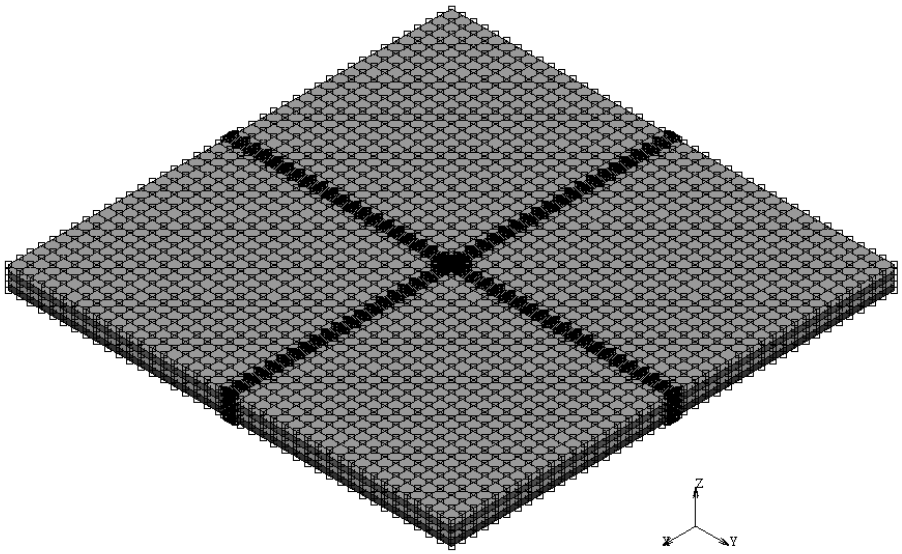

Fig. 3 2 km by 2 km numerical model of the soil below the heliport infrastructure

3.2 Wave attenuation: a second physical reduction

Once the height of the soil block under investigation is discretized into 5 layers only, a broad horizontal extension can be covered. Fig. 3) shows the mesh over a base square of 2 km by 2 km. Reduced models covering 1 km by 1km and 0.5 km by 0.5 km were also built and their response to an impact on the central top area was investigated. The comparisons carried out in (Marchese 2015) gave evidence that the model covering a square of 1 km by 1 km is not affected by reflection waves under the selected damping ranges.

3.3 Focusing on the response of interest

The heli-surface is designed in reinforced concrete and is a circular plate of diameter 50 m. For each impact scenario, the source event requires to define:

1) the impact location; for sake of simplicity, but without loss of generality, the impact on the centre of the heli-surface is studied.
2) the extension of the impact; a punctual impact is considered.
3) the generated pulse force. As shown in (Faravelli and Bigi 1990), it depends on the features of the two impacting deformable bodies. Since each helicopter type shows its own characteristics, the scenario must account for the worst situation, i.e., a duration of the pulse able to produce resonance in the system. Therefore, one assigns the mass of the helicopter, the height from where the fall starts and the associated velocity vector. Such data provide the impact impulse, assumed to have a triangular shape of duration 0.04 s for the case under investigation. The others data are: impacting mass 8600 kg, height 10 m and

vertical component of the velocity 10 m/s. From the impact impulse one obtains the vertical component of the impact force, to which a horizontal component of halved intensity is associated.

Fig. 4 provides the system response in term of acceleration time histories (vertical and horizontal along the axis *x* in Fig. 3) at different distances from the impact areas, when a low damping soil is considered. It is seen that significant values of the peak acceleration are reached. These FEA results were obtained by the software Marc (http://www.mscsoftware, 2004) on the model of size 1 km by 1 km and dense as the one in Fig. 3. Their values are lower in a better damped situation as the one of Fig. 5, but in the absence of accurate geo-gnostic analyses the designer has to conceive and implement solutions to reduce the peak acceleration.

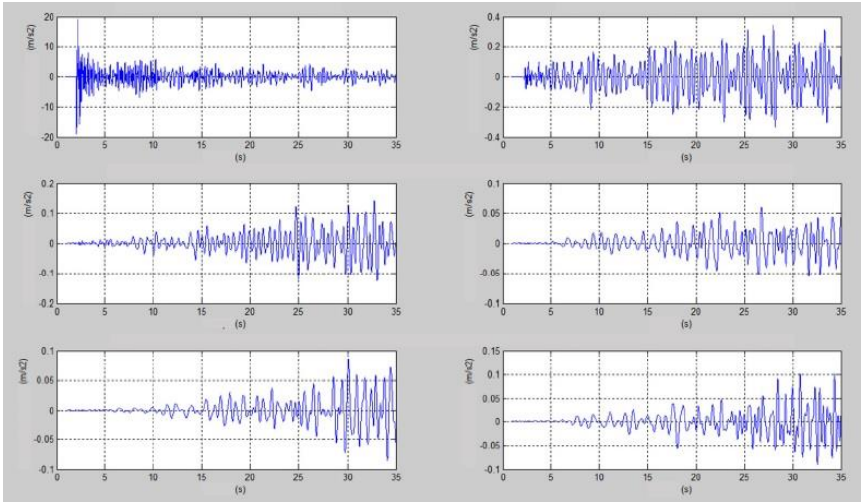

(a)

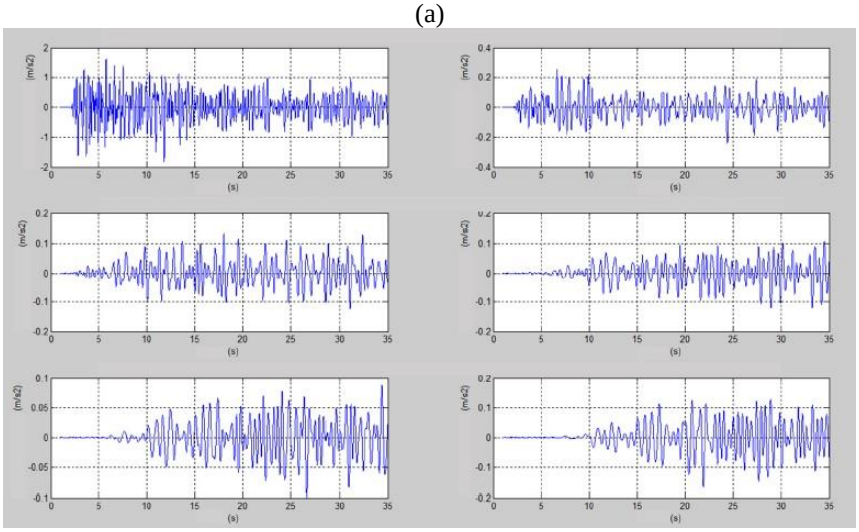

(b)

Fig. 4 Acceleration response at the impact zone and at a distance of 100, 200, 300, 400 and 500 m, respectively. Time histories of (a) vertical acceleration and (b) horizontal acceleration (the first plot is at 25 m from the impact point)

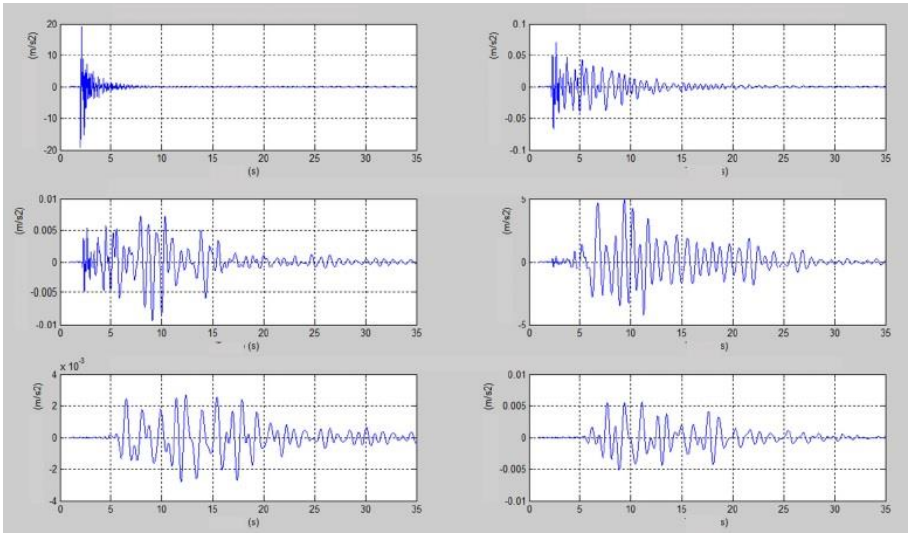

(a)

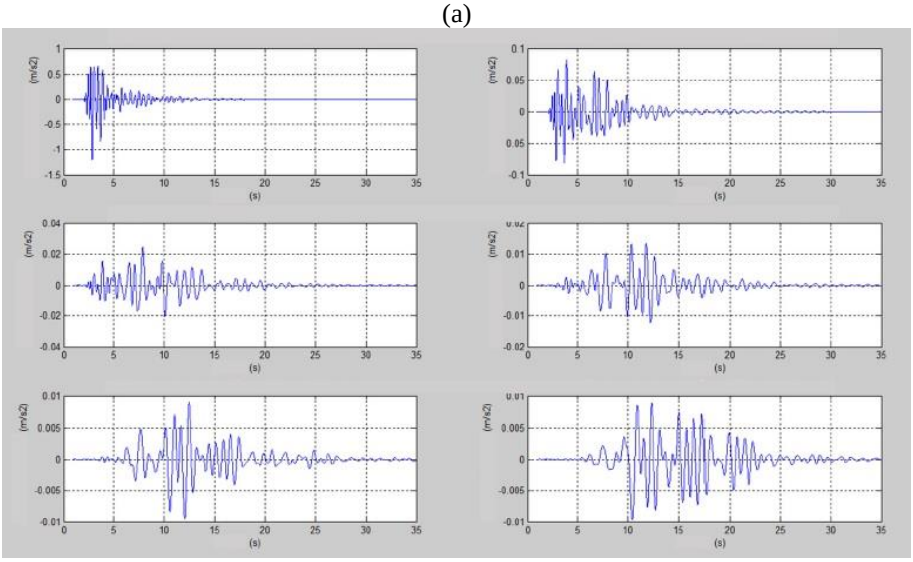

(b)

Fig. 5 Acceleration response, at the impact zone and at a distance of 100, 200, 300, 400 and 500 m, respectively, in a damped situation. Time histories of (a) vertical acceleration and (b) horizontal acceleration (the first plot is at 25 m from the impact point)

This can be achieved either by studying suitable isolation schemes or by introducing retaining barriers, which prevent the vibration wave to propagate in a direction, conveying it along the transversal direction. The result is achieved by building containment walls in the direction *y* of Fig. 3. Walls of the depth of two layers and of length of two times the heliport plate diameter are studied in that follows; the section is triangular with a basis of 0.8 m at the top. However, the

starting model of Fig. 6 is adopted, which is of the same size, but not so rich of nodes and elements, which were 4671 and 3508, respectively. The nodes are 1535 (including the walls' geometry), number which must be multiplied by the number of degrees of freedom per node (3) and by 2 to account for velocity and displacement. The result 9210 is then cleaned by those degrees of freedom which are constrained by geometric boundary conditions: 6716 is the actual number of involved degrees of freedom for the model of Fig. 6.

The authors are well aware that the model in Fig. 6 is not consistent with the one in Fig. 3, mainly for the reduced number of nodes to which boundary conditions are assigned. This is well illustrated by the comparisons of the response time histories summarized in Fig. 7. They are estimated in some nodes in the absence of walls and for the damped situation corresponding to Fig. 5. Nevertheless, the focus of this manuscript is on the potential of the mathematical model order reduction, rather than on the physical model order reduction. A more manageable starting model is therefore consistent with the purposes of the paper.

4. Reporting on the investigated design situations

From now on, the model incorporate the walls geometry and the damping is decreased by dividing the Rayleigh coefficients by a factor 10. Nevertheless, since the first step is to build the reduced order model from the one in Fig. 6 in the linear elastic case, the walls are in this stage regarded as made by linear elastic material. The theoretical background in (Casciati and Faravelli 2014) and (Casciati and Casciati 2016) provides the Hankel singular values in Fig. 8. This distribution was obtained assigning the matrix $\boldsymbol{C}$ for the whole set of displacements and velocities at the free nodes. Fig. 9 compares the horizontal (along x) displacement in node A of Figure 6, as obtained by the full model analysis (via the software Marc) and by the reduced models of 1367 and 145 state variables, respectively (via the software Matlab (http://www.mathworks , 2004)). It is seen that the smaller model, which shows nice manageability features, is quite inaccurate, but also the larger model is far from being accurate.

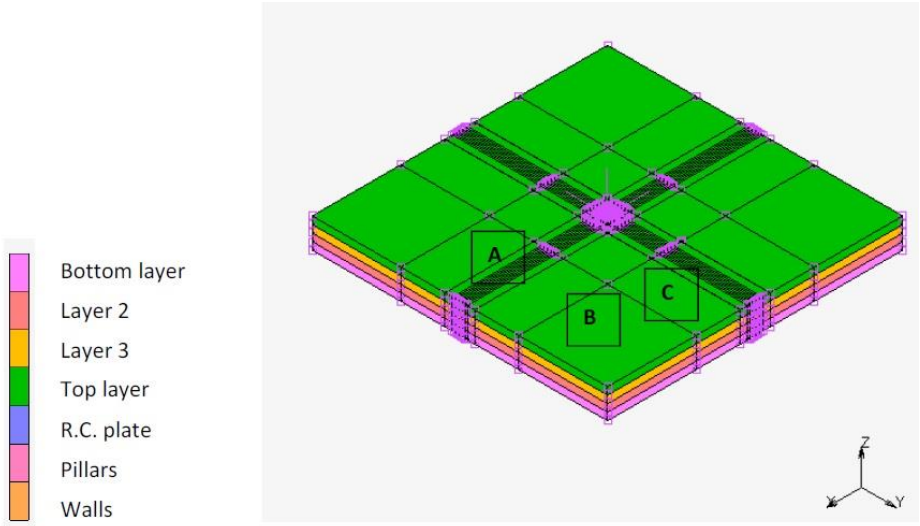

Fig. 6 Actual discretization adopted as starting point for the model reduction developments

4.1 Adjusting the linear reduced model manageability

Fig. 10 shows the same comparison when the reduced model is achieved from a matrix ***C*** which incorporates only 9 rows of that global matrix (the three components of the displacements in the nodes A, B and C in Fig. 6). It is seen that in this way the achieved accuracy is acceptable, thus allowing one to operate with a very modest number of degrees of freedom, i.e., 145 only.

Fig. 11 confirms that this conclusion still hold when further 330 rows are added to ***C***: those corresponding to the three degrees of freedom of the 110 nodes on the boundary of the walls. Indeed, the values of these displacements are the starting points for computing the interface forces (Eq. (14)). They are already included in the linear solution up to now obtained.

A further aspect left to future investigation is the disparity between the FEA solution tool and the one offered by the software environment Matlab (http://www.mathworks , 2004), within which the reduced order model is caught. The full model in Fig. 6, with no walls, requires a computational effort of 945 s in the MSC software for 6801 steps (0.14 s per step), to be compared with the 2990 sec required by the one adopted to obtain Figs. 4 or 5 , i.e., nearly 0.44 s per step.

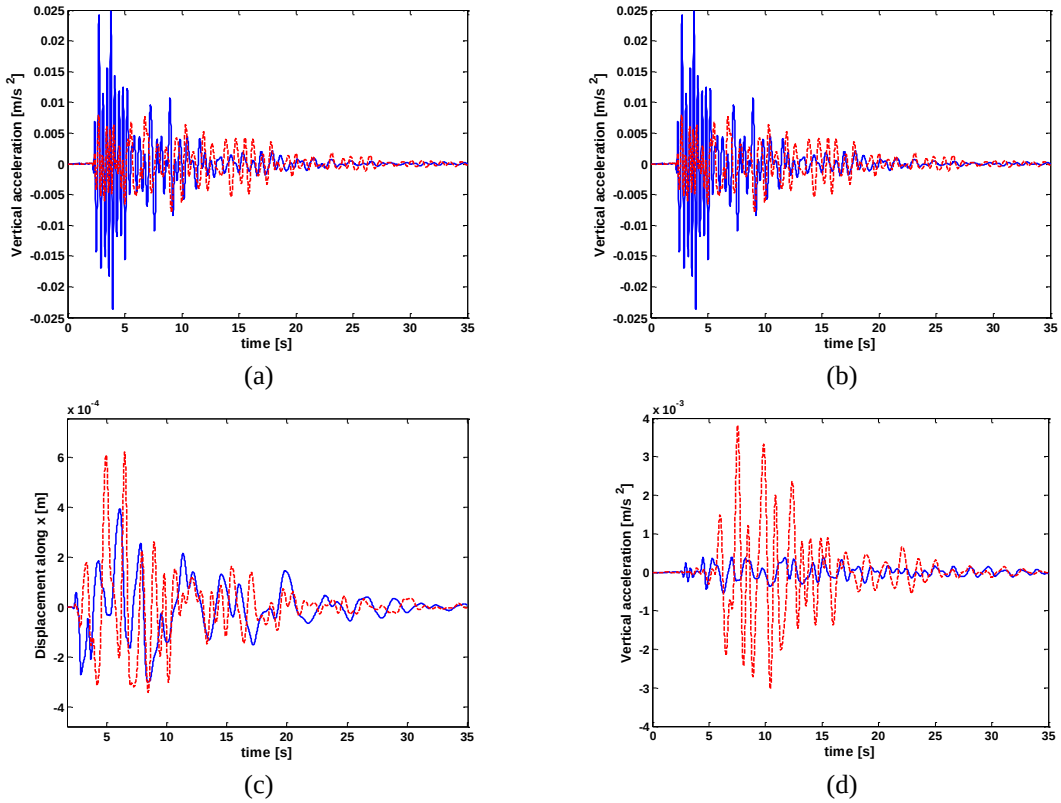

Fig. 7 Comparison of the response time histories estimated by the damped model of Fig. 6 (solid line) with those achieved by the damped model of Fig. 3 (dashed line). a) vertical acceleration in the axis point A in Fig. 6 (see third plot in Fig. 5(a)), (b) horizontal acceleration estimates at node A in Fig. 6 (see third plot in Fig. 5(b)), (c) horizontal displacement (along *x*) estimates at node A in Fig. 6 and (d) vertical acceleration estimates at node B in Fig. 6

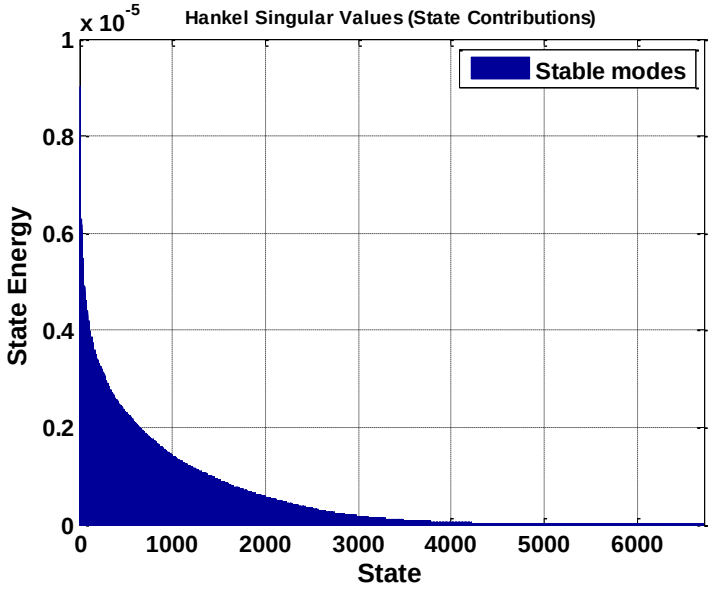

Fig. 8 Hankel singular values from the model in Fig. 6

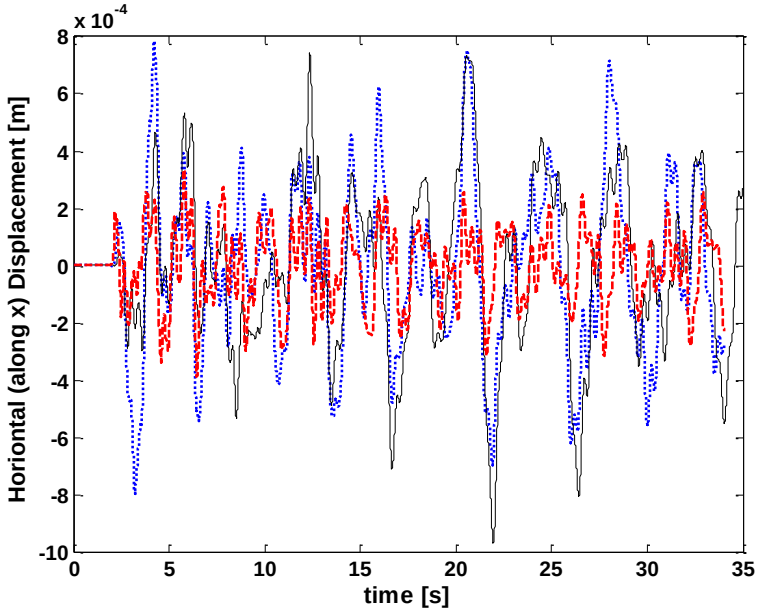

Fig. 9 Horizontal (along x) displacement estimates at node A from the linear model in Fig. 6: full model (solid line), reduced 1367-states model (dotted line) and its reduced 145-states model (dashed line). Full matrix $\boldsymbol{C}$.

Moving the model in Matlab it needs 600 s per step, which are reduced to 0.03 s per step in the model with 145 states. Thus it would be very fascinating the chance of re-importing the reduced order model in the MSC software.

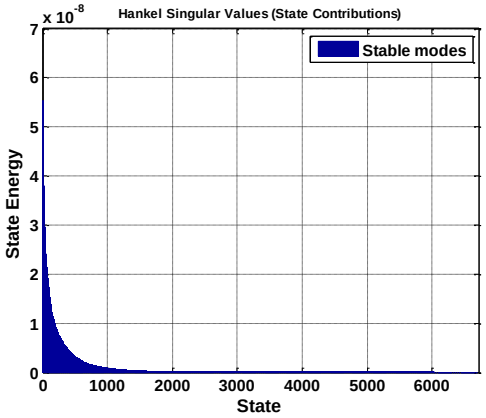

(a)

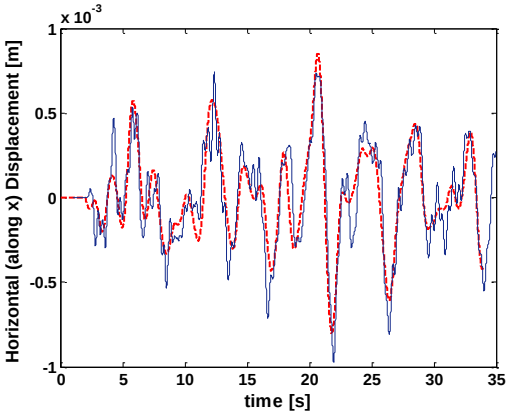

(b)

Fig. 10 (a) Hankel singular values from the model in Fig. 6 and (b) Horizontal (along *x*) displacement estimates at node A from the linear model in Figure 6: full model (solid line), and its reduced 145-states model (dashed line). Matrix ***C*** of 9 rows only

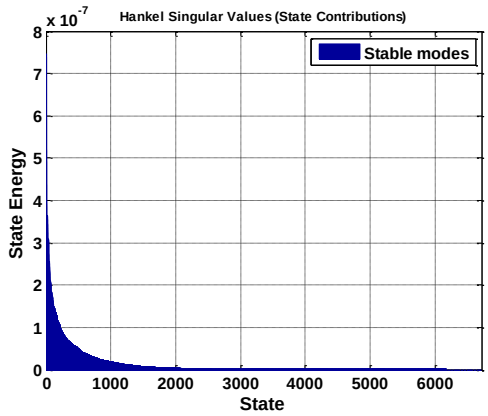

(a)

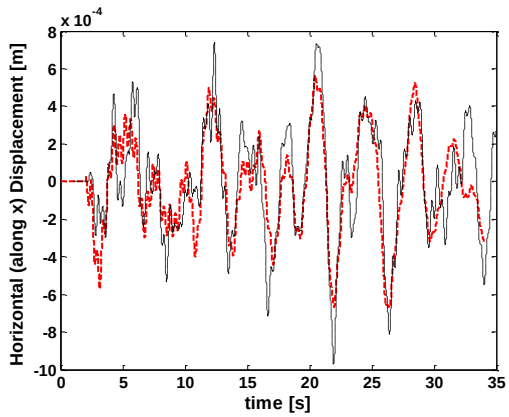

(b)

Fig. 11 (a) Hankel singular values from the model in Fig. 6 and (b) Horizontal (along *x*) displacement estimates at node A from the linear model in Fig. 6: full model (solid line), and its reduced 145-states model (dashed line). Matrix ***C*** of 339 rows

4.2 Quantifying the effect of the presence of linear walls

Fig. 12 emphasizes the presence of linear walls in the numerical model of Fig. 6. The time histories of the horizontal acceleration in point A and those of the vertical accelerations in points A, B and C obtained with and without walls are compared each with the other. It is seen the beneficial effects of the walls presence in points A and B, while there is not any deterioration in point C.

Fig. 12 compares displacements for which the reduction synthesized in Fig. 11 works well in preserving the accuracy. But, comfort issues are ruled by accelerations. To rely on a consistent accuracy on them, one has to modify again the reduction scheme, by introducing in matrix $\boldsymbol{C}$ 6 further rows per each of the three nodes A, B and C, i.e., the components of velocities and accelerations. The last ones generally requires the specification of matrix $\boldsymbol{D}$ in Eq. (2) and, hence, the knowledge of the excitation time history. Fig. 13 provides the relevant Hankel singular values and an example of acceleration comparison. Starting from this linear reduced order method (with 357 rows in matrix C), one can start the extension to wall in nonlinear material following the formulation summarized in Eqs. (11)-(14).

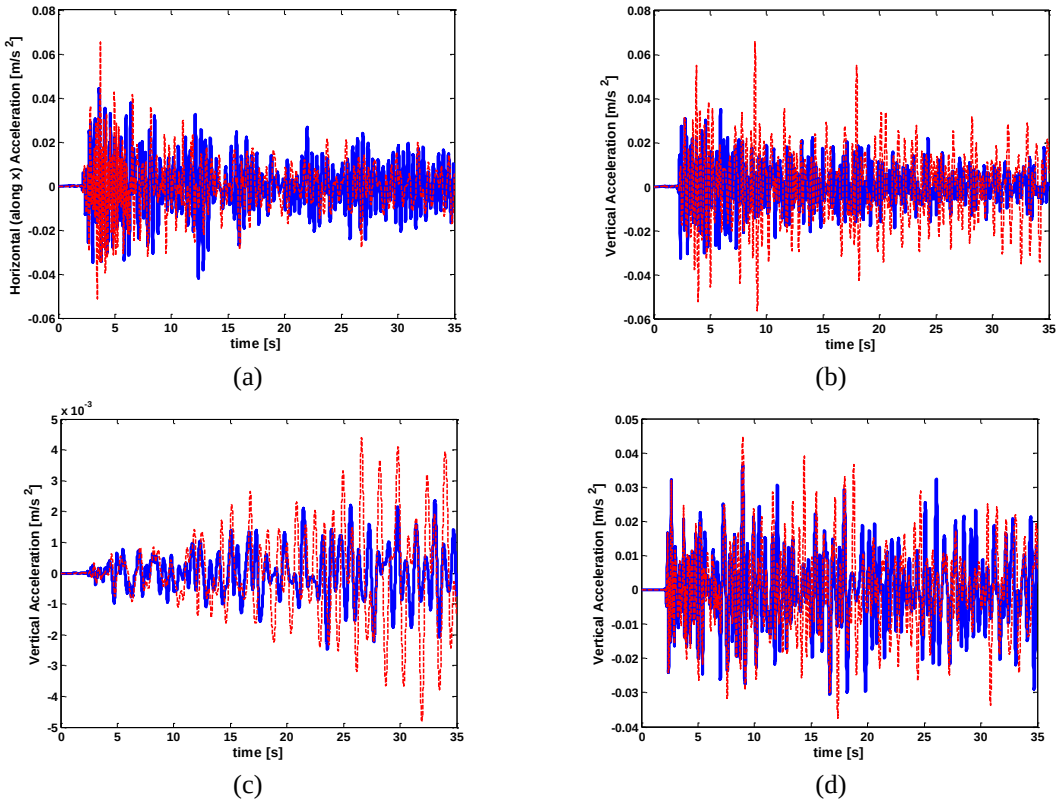

Fig. 12 Horizontal (along *x*) acceleration in point A; Vertical accelerations in points (b) A, (c) B and (d) C. Time histories without (dashed line) and with (solid line) the walls

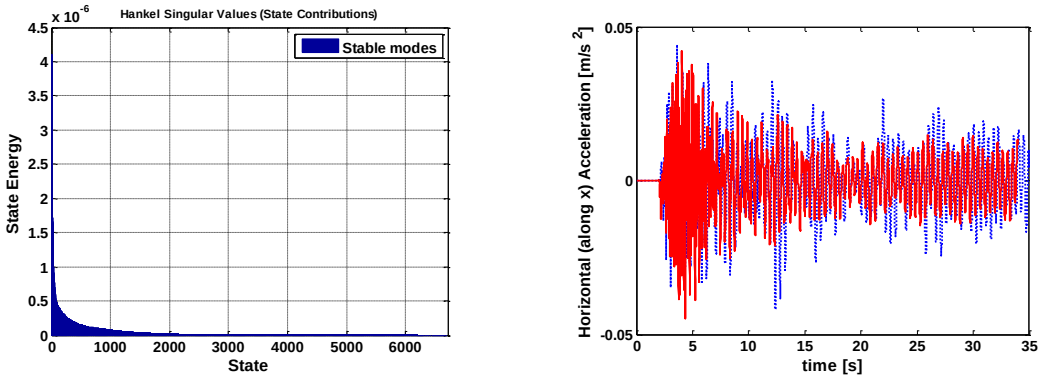

(a) (b)

Fig. 13 (a) Hankel singular values from the model in Fig. 6, (b) Horizontal (along x) acceleration estimates at node A from the linear model in Fig. 6: full model (dotted line), and its reduced 145-states model (solid line). Matrix C of 357 rows, i.e., 339 as in Fig. 11 plus 18

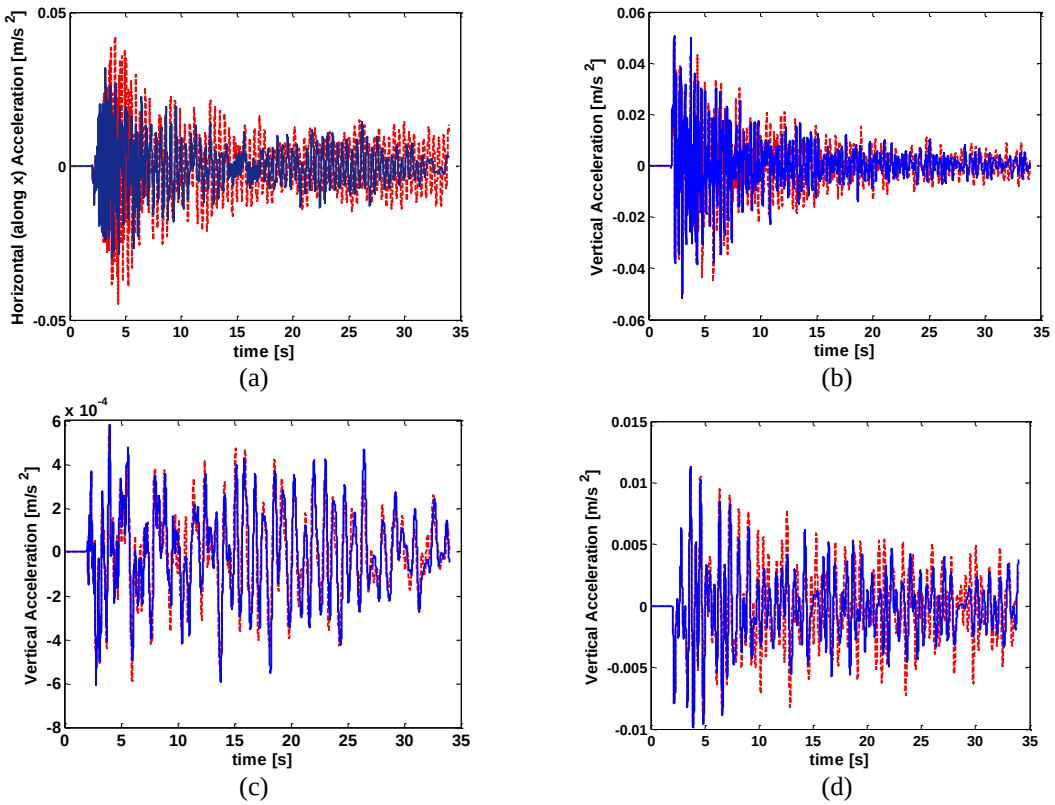

(a) (b) (c) (d)

Fig. 14 (a) Horizontal (along *x*) acceleration in point A; Vertical accelerations in points (b) A, (c) B and (d) C. Time histories from the reduced order model (145 states) for linear walls (dashed line) and from the reduced order model rearranged to account for the wall material nonlinearity (solid line).

4.3 Adopting nonlinear material walls

The transient dynamic analysis leading one to estimate the system response operates by time steps. At each step one computes the ratio ζ of the absolute value of each displacement component in every wall border node with a limit value, say 0.005 m. If the ratio is higher than 1, the corresponding column entries k_d of the walls' stiffness matrix are put equal to 10% of their original value k. Otherwise each matrix entry k is rearranged in k_d by a linear interpolation . Of course any other equation can be incorporated in the numerical model and the structural response simulated.

The results are shown in Fig. 14, where they are compared with the linear solution to assess the suitability of designing the walls in such a nonlinear way.

5. Conclusions

Several civil engineering problems require rather extended numerical models since truncations could results in undesired phenomena. Most of this large dimension problems can be treated in a linear environment and, hence, standard simple techniques of model order reduction (MOR) apply in view of long transient dynamic analyses. When nonlinear components are incorporated, however, these MOR technique cannot be used and the alternative would be to exploit MOR schemes for nonlinear problems, which are generally rather cumbersome.

In this paper it is shown how to use standard MOR techniques in those cases that include rather limited extension of nonlinear components. This is the case of retaining barriers used to prevent the wave propagation induced by impact. The proposal is exemplified for one of the impact scenarios that should be studied in the design process of a urban heliport.

Acknowledgments

The authors acknowledge the athenaeum research grant from the University of Pavia on which the met expenses were charged.

References

Basu, B., Bursi, O.S., Casciati, F. *et al.* (2014), "A European association for the control of structures joint perspective. Recent studies in civil structural control across Europe", *Struct. Control Health Monit.*, **21**(12), 1414-1436.

Casciati, F, and Casciati, S. (2006), "Structural health monitoring by Lyapunov exponents of non-linear time series" , *Struct. Control Health Monit.*, **13**(1), 132-146.

Casciati, F. and Casciati, S. (2016), "Designing the control law on reduced-order models of large structural systems", *Struct. Control Health Monit.*, **23**(4) ,707-718.

Casciati, F. and Faravelli, L. (1991), *Fragility analysis of complex structural systems*, Research Studies Press, Taunton, UK.

Casciati, F. and Faravelli, L. (2012), "Model order reduction issues for integrated structural control design", *Adv. Sci. Technol.*, **83**, 37.

Casciati, F. and Faravelli, L. (2014), "Sensor placement driven by a model order reduction (MOR)

reasoning", *Smart Struct. Syst.*, **13**(3), 343-352.
Casciati, S. (2014), "Differential evolution approach to reliability-oriented optimal design", *Probab. Eng. Mech*., **36**, 72-80.
Casciati, S. and Borja, R.L. (2004), "Dynamic FE analysis of south Memnon colossus including 3D soil-foundation-structure interaction", *Comput. Struct*., **82**(20-21), 1719-1736.
Casciati, S. and Faravelli, L. (2014), "Quantity vs. quality in the model order reduction (MOR) of a linear system", *Smart Struct. Syst.*, **13**(1), 99-109.
Casciati, S. and Osman, A. (2005), "Damage assessment and retrofit study for the Luxor Memnon colossi", *Struct. Control Health Monit.*, **12**(2), 139-156.
Casciati, S., Chassiakos, A.G. and Masri, S.F. (2014), "Toward a paradigm for civil structural control", *Smart Struct. Syst.*, **14**(5), 981-1004.
Faravelli, L. and Bigi, D. (1990), "Stochastic finite-elements for crash problems", *Struct. Saf.*, **8**(1-4), 113-130.
Farhat, C., Avery, Ph., Chapman, T. and Cortial, J. (2014), "Dimensional reduction of nonlinear finite element dynamic models with finite rotations and energy-based mesh sampling and weighting for computational efficiency", *Int. J. Numer. Meth. Eng.*, **98**(9), 625-662.
Farhat, C., Chapman, T. and Avery, Ph. (2015), "Structure-preserving, stability, and accuracy properties of the energy-conserving sampling and weighting method for the hyper reduction of nonlinear finite element dynamic models", *Int. J. Numer. Meth. Eng*, **102**(5), 1077-1110.
http://fas.org/nuke/intro/aircraft/afman32-1123.pdf (1999)
http://www.faa.gov/documentlibrary/media/advisory_circular/150-5390-2b/150_5390_2b.doc (2004)
http://www.mathworks.com/index.html?s_tid=gn_loc_drop (2004)
http://www.mscsoftware.com/it/product/marc (2004)
https://www.wbdg.org/ccb/DOD/UFC/ufc_3_260_01.pdf (2008)
Marchese, R. (2015), *Propagazione spazio-temporale degli effetti di un'esplosione (in Italian)*, Civil Engineering Master Thesis, University of Pavia.